Near Surface Geophysics, 2016, **14**, xxx-xxx doi:10.3997/1873-10.3997/1873-0604.2016007

Suitable real-time monitoring of the aerobic biodegradation of toluene in contaminated sand by spectral induced polarization measurements and CO_2 analyses

Cécile Noel[1,2*], Jean-Christophe Gourry[1], Jacques Deparis[1], Ioannis Ignatiadis[1], Fabienne Battaglia-Brunet[1] and Christophe Guimbaud[2]

[1] *French Geological and Mining Research Centre (BRGM), 45100 Orléans, France*
[2] *Physical and Chemical Laboratory of Environment and Space (LPC2E), CNRS, 45071 Orléans, France*

Received July 2014, revision accepted December 2015

ABSTRACT

Hydrocarbons commonly contaminate aquifers and, in certain cases, can be successfully treated through biodegradation. Biodegradation is an effective technique for cleaning up pollution by enhancing pollutant-degrading bacteria *in situ*. However, *in situ* sampling for monitoring processes occurring into the ground during the treatment is expensive and invasive. In this article, an alternative method was tested. Spectral Induced Polarization (SIP) was combined with gas analyses, CO_2 concentration and its carbon isotopic ratio, to monitor toluene aerobic biodegradation in laboratory columns. Microbial activity was characterized by an evolution of the SIP response in correlation with a CO_2 production with the same carbon isotope signature as toluene. The spectral induced polarization response followed the variations of bacterial activity and displayed a phase shift up to 15 mrad. These results support the feasibility of using geophysical measurements, supported by CO_2 analyses, to monitor *in situ* hydrocarbon biodegradation, and they are proving to be highly promising for real field scale monitoring.

INTRODUCTION

Petroleum hydrocarbon leaks and accidental spills commonly happen during the production, refining, transport, and storage of petroleum. Release of petroleum hydrocarbons into the environment causes damage to ecosystems (Das and Chandran 2011) and to soil and water resources (Nadim *et al*. 2000). Increasing demand for drinking water and cropland with population growth requires effective remediation techniques to treat the contamination and to decrease hostile effects on health and environment.

Microbial degradation can be considered as a major component in the petroleum hydrocarbon remediation approach (Das and Chandran 2011). The process of *in situ* bioremediation enhances the activity of the indigenous bacteria of the aquifer to detoxify or remove pollutants (Weiss and Cozzarelli 2008). This process is an effective way to clean up pollution, even though bioremediation is relatively time consuming. In addition, *in situ* bioremediation technology is very promising as being often cost effective and environmentally friendly compared with conventional *ex situ* techniques (Majone *et al*. 2014). Nevertheless its potential remains partially unexploited, mainly because *in situ* monitoring during and after soil treatment operations is often expensive and technically challenging (Hyman and Dupont 2001; Davis *et al*. 2013). Indeed, where significant subsurface heterogeneity exists, conventional intrusive groundwater sampling campaigns can be insufficient to obtain relevant information as they are restricted to costly monitoring wells at discrete locations, with no information between sampling points (Commission Directive 2014/80/EU). New monitoring tools are needed to overcome these limitations and make the *in situ* bioremediation more reliable, robust, and economically competitive.

Geophysical tools, particularly induced polarization (IP) method, are suitable to detect hydrocarbon contamination (Towle *et al*. 1985; Olhoeft 1986; Vanhala 1997; Sogade *et al*. 2006; Flores Orozco *et al*. 2012) and to study the effects of biodegradation processes (Sauck 2000; Abdel Aal *et al*. 2004; Abdel Aal, Slater, and Atekwana 2006; Williams *et al*. 2009; Atekwana and Atekwana 2010; Heenan *et al*. 2013; Mewafy *et al*. 2013; Abdel Aal and Atekwana 2014). Indeed, the saturation and physicochemical properties of hydrocarbons are factors that affect the IP signature of contaminated soils (Cassiani *et al*. 2009; Ustra *et al*. 2012). Oil wettability is rather important: quadrature conductivity seems to be competitively controlled by (i) the insulating nature of the oil phase and (ii) the surface area (interphase) between the oil phase and the water phase, especially for very

* E-mail: cecile.noel@cnrs-orleans.fr

non-wetting oil (Schmutz *et al*. 2010; Schmutz, Blondel, and Revil 2012; Revil, Schmutz, and Batzle 2011; Abdel Aal and Atekwana 2014).

Biodegradation processes modify electrical properties as well because they alter biogeochemical conditions for many reasons (Atekwana and Slater 2009). In several studies, spectral IP (SIP) measurements on samples undergoing hydrocarbon biodegradation presented a higher magnitude of imaginary conductivity and phase shift compared with uncontaminated samples (Abdel Aal *et al*. 2006; Personna *et al*. 2013). Indeed, bacteria alter local redox conditions and produce new redox gradients (Naudet and Revil 2005); microbial activity can induce precipitation of sulfides (sulfate-reducing bacteria) and produce organic acids (acetogenic or lactogenic bacteria) that affect pore water conductivity (Personna *et al*. 2008; Schwartz, Shalem, and Furman 2014); during microbial growth and formation of biofilms, biomass can clog pores and potentially change porosity and hydraulic conductivity (Ntarlagiannis, Yee, and Slater 2005; Davis *et al*. 2006; Ntarlagiannis and Ferguson 2009; Albrecht *et al*. 2011).

Moreover, other studies show that bacteria have a direct impact on electrical properties and suggested that the electrical signatures of bacterial suspensions are not only due to the bacterial modifications of the geological media but that it may also be directly linked to bacteria themselves (Yang 2008; Zhang, Slater, and Prodan 2013). Revil *et al*. (2012) proposed a model of the bacteria SIP response by comparing it to clay minerals coated with electrical double layer with high ionic mobility. Therefore, it seems possible to infer growth rate of bacteria in porous sand from induced polarization measurements.

According to these studies, IP could be an effective non-intrusive tool to monitor bioremediation. Moreover, geoelectrical measurements are often used in conjunction with geochemical methods (mainly, temperature, pH and redox potential measurements, electrical conductivity, and dissolved oxygen content for example) to detect changes in the chemical properties of the geologic media caused by microbial metabolism. On the field scale, these geochemical measurements often imply an access to the fluid and/or samples by using monitoring wells. To propose a complete non-destructive monitoring methodology, we introduce here a technique to follow microbial metabolism by studying gas emissions at the surface of the geologic media. Indeed, biodegradation of organic compounds induces the production of CO_2 (Kaufmann *et al*. 2004; Sihota, Singurindy, and Mayer 2011), which may be distinguished from that produced by other processes based on the carbon isotopic compositions characteristic of the source material and/or fractionation accompanying microbial metabolism (Sihota and Mayer 2012). Indeed, carbon isotopic signature of CO_2 reaches that of contaminant (Aggarwal and Hinchee 1991), and it can be accompanied by significant carbon isotope fractionation: inorganic carbon produced by bacteria can be depleted in ^{13}C as compared with the initial isotopic ratio of carbon source, whereas the produced biomass is enriched in ^{13}C (Hunkeler *et al*. 2001). Some studies evaluated carbon isotope fractionation during biodegradation of hydrocarbons as a possible tool to trace the process in contaminated environments (Meckenstock *et al*. 2004; Elsner 2010; Morasch *et al*. 2011), but they mainly deal with analyses on residual pollutants not on produced CO_2. One of the objectives of this contribution is to assess CO_2 efflux measurements and isotopic analysis to evaluate biodegradation processes.

Our work is aimed to provide a comprehensive laboratory-scale characterization of hydrocarbon biodegradation process by means of both SIP measurements and gas analyses (volumetric concentration and carbon isotopic ratio). This integrated approach tends to develop a new non-invasive technique for monitoring *in situ* biodegradation of hydrocarbons. Laboratory experiments are a necessary step to evaluate the feasibility of this monitoring methodology. To this end, aerobic microbial activity of the strain *Rhodococcus wratislaviensis* IFP 2016 was monitored in toluene-contaminated sand columns. Indirect information coming from SIP measurements and CO_2 gas analyses are validated by direct measurements of physicochemical parameters, evaluation of the remaining toluene amount, and counts of bacterial populations.

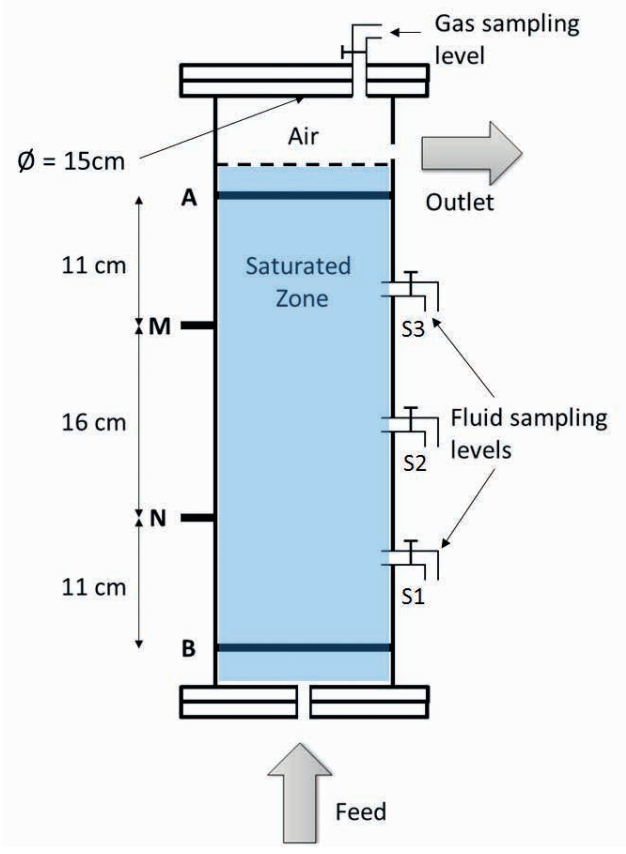

Figure 1 Column design. (Left) SIP measurements disposal: A and B are MP35N ring current electrodes; M and N are handicraft $Cu/CuSO_4$ point potential electrodes. (Right) Gas sampling point at the top of the column, fluid sampling points at three different heights. The column is fed up with bacterial growth medium and toluene.

EXPERIMENTAL SETUP

Column design, packing, and operating conditions

Columns (Fig. 1) were 50 cm long and constructed from a 15-cm-diameter polyvinylidene difluoride (PVDF or Kynar®) tube. It is a highly non-reactive polymer generally used in applications requiring resistance to solvents (Schweitzer 2004).

Columns were dry-packed with Fontainebleau sand (France) over 45 cm, which is the overflow level (Fig. 1). The last top 5 cm of the column was an empty zone kept for CO_2 degassing. Sand porosity Φ is determined by weighing the sand volume before and after saturation with deionized water, and it is found to be equal to 39.16 ± 0.03%. The value of porosity is checked by a tracer experiment (conductimetric detection), validated by a 1D PHREEQC simulation (Parkhurst and Appello 1999): a high-conductivity KCl solution (0.1 M) is injected at constant flow rate at column entry and detected at column outlet by a conductivity probe. This experiment allows determining the retention time of the system at a given flow rate, the retention volume is deduced, and porosity is calculated knowing the sand and column volumes. The two methods give the same results. Fontainebleau sand (Sibelco, France) was characterized by the manufacturer: its D_{50} is equal to 209 µm, and its chemical composition is as follows: 99.83% SiO_2 (essentially quartz), 0.017% Fe_2O_3, 0.050% Al_2O_3, 0.017% TiO_2, 0.007% CaO, and 0.005% K_2O. The sand was washed with deionized water and sterilized by autoclaving prior to being packed in the columns. We performed three cycles at 24-hour interval in order to eliminate the sporulated microorganisms. Each autoclaving phase eliminates the active cells but not entirely the spores, which can become active cells in the 24-hour interval between autoclaving. Sterile conditions were maintained by two Bunsen burners while packing. Columns and tubing were disinfected with 90% ethanol and rinsed with sterilized water.

Two columns were used in this experiment. One non-inoculated was used for control measurements, and one inoculated was used for biodegradation monitoring.

Both columns were fed up with toluene (C_7H_8), a major component of gasoline and diesel oil, and the bacterial growth medium rich in vitamins, oligo elements, and mineral salts ($MgSO_4$: 0.5 $g.L^{-1}$; NH_4NO_3: 1.5 $g.L^{-1}$; $CaCl_2$: 0.04 $g.L^{-1}$; and potassium phosphate KH_2PO_4/K_2HPO_4 buffer solution). The inoculated column was inoculated with a *Rhodococcus wratislaviensis* (*R. wratislaviensis*) IFP 2016 bacterial culture. *R. wratislaviensis* is known to be a toluene-degrading strain: in the presence of oxygen, toluene is oxidized to carbon dioxide (CO_2) and water during bacterial metabolism (Auffret *et al*. 2009). The inoculum (around 10^5 bact/mL) was introduced in the feeding solution, and it was left recirculating in closed loop during five days (inoculation step). Then, the circuit was opened (circuit opening), and the column was supplied with fresh sterile medium spiked with H_2O_2 in low concentration to stimulate aerobic metabolic bioprocesses. The columns were kept in a climate chamber at 25 °C.

The columns were fully equipped for several measurements (Fig. 1). On the left, for SIP measurements, two ring MP35N (nickel–cobalt alloy: 35% Ni, 35% Co, 20% Cr, and 10% Mo) current electrodes were installed 38 cm apart at both ends of the column. MP35N alloy is a nonmagnetic alloy possessing an excellent corrosion resistance. It had been used as nonmagnetic electrical components and instrument parts in medical, seawater, oil and gas well, chemical and food processing environments (Lessar *et al.* 2006) and as a current electrode material for SIP measurements (Oshetski 1999). Moreover, MP35N is used in the medical industry because it does not react with biological cells (Oshetski 1999), making it suitable for studying biological processes. In addition, two non-polarizable custom-made $Cu/CuSO_4$ potential electrodes (16 cm apart) were installed between the current electrodes. Gas was sampled with a syringe at the top of the column, and CO_2 gas concentration and carbon isotopic ratio of this CO_2 are both measured by infrared laser spectroscopy. Planktonic bacterial population and toluene concentration could be followed by sampling water at three levels of the columns (S1, S2, and S3). Moreover, sessile bacterial population was monitored through sand sampling at the top of the inoculated column.

Spectral induced polarization measurements

Spectral induced polarization (SIP) or complex resistivity method measures the frequency dependence of complex impedance between few millihertz and kilohertz. Complex impedance could be associated to electrochemical charge migration and accumulation at the fluid–mineral interface, known as the electrical double layer (EDL) (Kemna *et al.* 2012). Initially developed for mineral exploration (Bleil 1953), the SIP method is more and more applied for environmental investigations (Olhoeft 1986; Vanhala 1997; Sogade *et al*. 2006; Flores Orozco *et al*. 2012).

The SIP method is sensitive to changes in pore fluid chemistry, porosity, and mineral–fluid interface properties (Kemna *et al.* 2012). All of these parameters can be potentially altered by microbial activity. Moreover, bacterial cells are negatively charged (Revil *et al*. 2012) and form an additional interface (EDL) in contact with fluid. This can also generate a polarization response (Zhang *et al*. 2013).

SIP measurements (fundamental frequencies between 63 mHz and 128 Hz and their first two odd harmonics) were obtained by using a four-electrode disposal using a GDP 32II instrument from Zonge International (Tucson, AZ, USA). It is a multifunction receiver usually used for field electrical acquisition (Williams *et al*. 2009) and rarely in its Lab Roks mode for SIP laboratory experiments.

A square current (i.e., fundamental frequency and odd harmonics) is injected through two ring electrodes (MP35N, nickel–cobalt alloy) by the Laboratory Downhole Transmitter (LDT-10) from Zonge International. It can provide precision current-regulated frequency waveforms with amplitudes ranging from 1 µA

to 10mA. The induced voltage is measured through two other electrodes (custom-made $Cu/CuSO_4$, according to Maineult, Bernabé, and Ackerer 2004) by signal receiver/analyser GDP 32II from Zonge International.

The complex resistivity is related to the measured complex impedance by a geometrical factor . It is recorded as resistivity magnitude and phase shift (between the measured voltage and the impressed current) (equation (1)) (Reynolds 2011):

$$\rho^*(\omega) = kZ^*(\omega) = \frac{U}{I}k = |\rho^*(\omega)|e^{i\phi(\omega)} \quad (1)$$

where ω is the angular frequency and $i=\sqrt{(-1)}$. The resistivity magnitude $|\rho^*(\omega)|$ represents ohmic conduction (capacity to conduct current), whereas phase shift ϕ describes polarization strength (charge storage).

Note that the phase sign of resistivity is negative as the measured potential U is delayed from the imposed current I. The complex conductivity σ^* is the reverse of complex resistivity (Personna *et al*. 2013; Slater and Lesmes 2002).

Geophysical system is checked by measuring complex electrical resistivity of a column filled with salted water (KCl 1 g/L, σ_w = 2050 µS/cm). Full spectra of the phase shift and resistivity are shown in Fig. 2. A constant phase shift is found around 1 mrad, with no variation between 0.25 Hz and 10 Hz. The error (standard deviation of six measurements) is lower than 0.9 mrad at these frequencies. Resistivity spectrum is constant at each frequency (between 63 mHz and 1000 Hz), with an error lower than 0.02 Ωm (Fig. 2).

In order to determine the formation factor F of Fontainebleau sand (see Archie's law (1942), equation (2)), the electrical resistivity of a sand column is measured as a function of water electrical resistivity in the range of 0.5 Ωm–100 Ωm (Table 1):

$$\rho = F\rho_w = \Phi^{-m}\rho_w \quad (2)$$

where Φ is the porosity and m the cementation exponent. Electrical measurements yield a formation factor F of 3.9. Knowing the sand porosity (Φ = 39%), we calculate the cementation factor m = 1.4.

During the experiments, the electrical measurements were performed once a day at the beginning (during one week) and then three times a week for the duration of the experiment (60 days for the inoculated column and only 15 days for the non-inoculated column, because aseptic conditions could not be maintained any longer). Experimental accuracy in the electrical measurements was calculated by averaging the electrical data for six stacks per frequency and calculating the standard deviation from the average.

At the end of the inoculated experiment, we repeated the measurement of formation factor F (electrical resistivity of sand

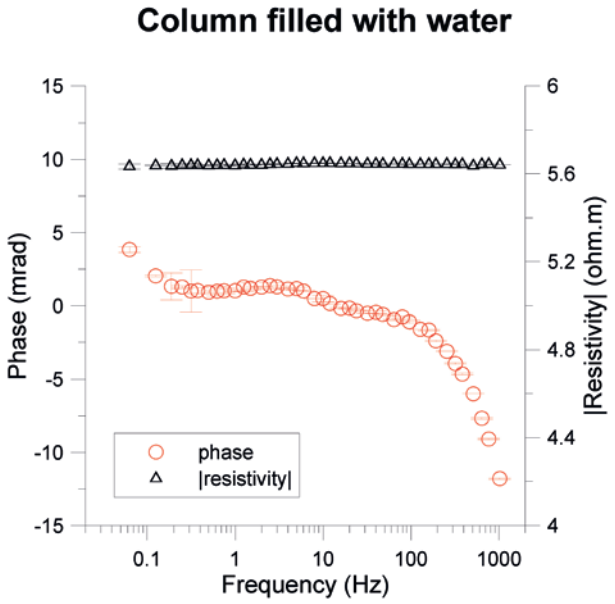

Figure 2 Full spectra of the phase shift between the injected current and the measured voltage (red circles) and resistivity (black triangles) measured in a column filled with salted water (KCl 1 g/L; σ_w = 2050 µS/cm).

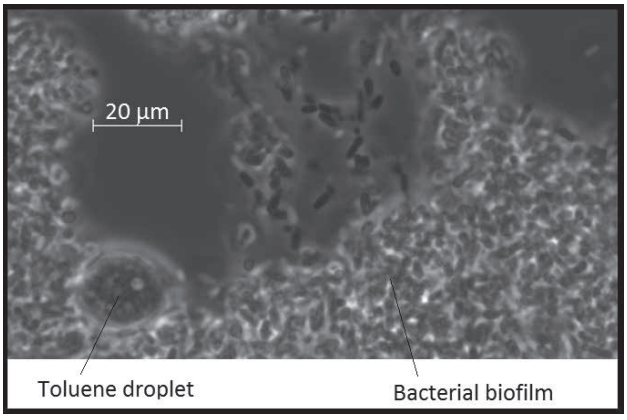

Figure 3 Optical microscope photograph of the biofilm detached from the sand at the top of the inoculated column (day 22). Biofilm seems to include a toluene droplet.

Table 1 Data used for calculation of formation factor F of the Fontainebleau sand: before the inoculated experiment (day 0, F = 3.9) and at the end of the experiment (day 58, F = 4.6).

	Day 0				Day 58		
Fluid resistivity ρ_ω (ohm.m)	83.3	13.6	10.9	0.76	7.1	3.7	1.71
Saturated sand resistivity ρ (ohm.m)	325.1	54.6	40.1	3.29	32.5	16.28	7.78
Formation factor F	3.9				4.6		

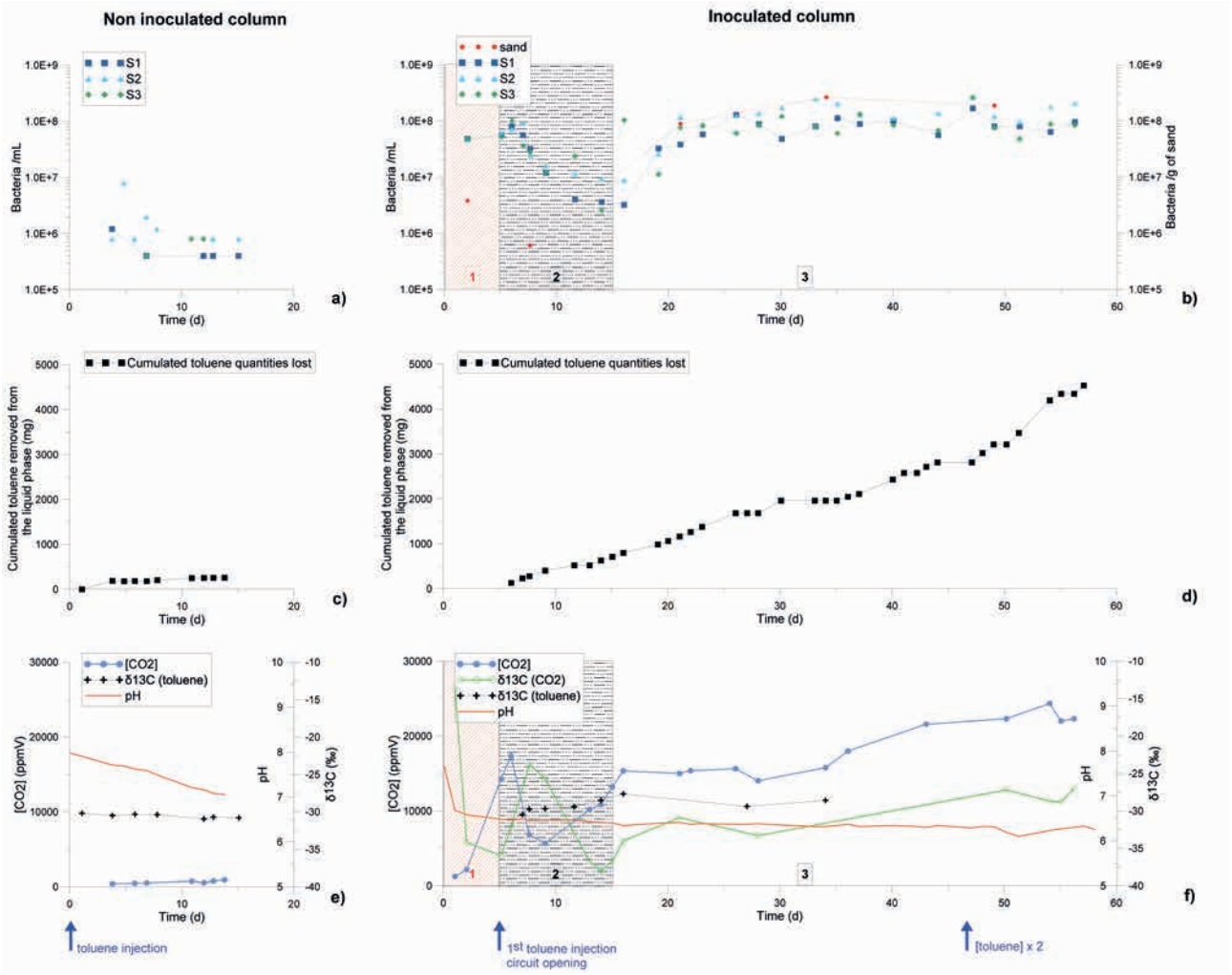

Figure 4 Microbial and geochemical results for the non-inoculated (left) and inoculated (right) columns of the measured (a and b) bacteria cell concentrations; (c and d) cumulated toluene quantities lost in liquid phase; and (e and f) CO_2 concentration, carbon isotopic ratio, and pH. Areas 1, 2, and 3 correspond to the inoculation period (days 0–5), the period when bacteria were lost after opening circuit (days 5–15), and the period of biofilm growth (days 15 to the end). Note that there are no carbon isotopic ratio measurements from CO_2 in the non-inoculated column due to the very low CO_2 concentrations.

column is measured as a function of the electrical resistivity of the electrolyte; see equation (2) and Table 1). It gives information on sand porosity evolution.

Geochemical and microbiological analyses

Infrared laser spectroscopy

CO_2 concentration and its isotopic ratio were measured by infrared laser spectroscopy. The spectrophotometer used was developed by the Physical and Chemical Laboratory of Environment and Space (LPC2E), CNRS, Orléans, France, and is a modified version of the SPectrometer InfraRed In Situ Tropospheric (SPIRIT), transportable transportable infrared spectrometer described in Noel *et al.* (2016), Guimbaud *et al*. (2016, 2011) and Gogo *et al*. (2011).

Carbon isotopic ratio $\delta^{13}C(CO_2)$ is calculated by equation (3) where R stands for the ratio $^{13}C/^{12}C$ and the sample ratio R_{sample} is compared with those of a standard, the Vienna Pee Dee Belemnite ($R_{standard}$= 1.2372‰):

$$\delta^{13}C\left(‰\right) = 1000\frac{\left(R_{sample} - R_{standard}\right)}{R_{standard}} \quad (3)$$

Sampling and analyses

CO_2 gas analyses were made daily and then twice a week. Gas (approximately 15 mL) was sampled with a syringe at the top of the column and injected in the SPIRIT to be analysed.

Calibration of SPIRIT is performed with a certified CO_2 gas cylinder (Air Liquide®): $[CO_2]$= 390 ppm, $\delta^{13}C(CO_2)$ = -43.2‰ obtained by Isotope-Ratio Mass Spectrometry (IRMS). Precision and accuracy of SPIRIT are higher than 0.3‰. Calibrations are

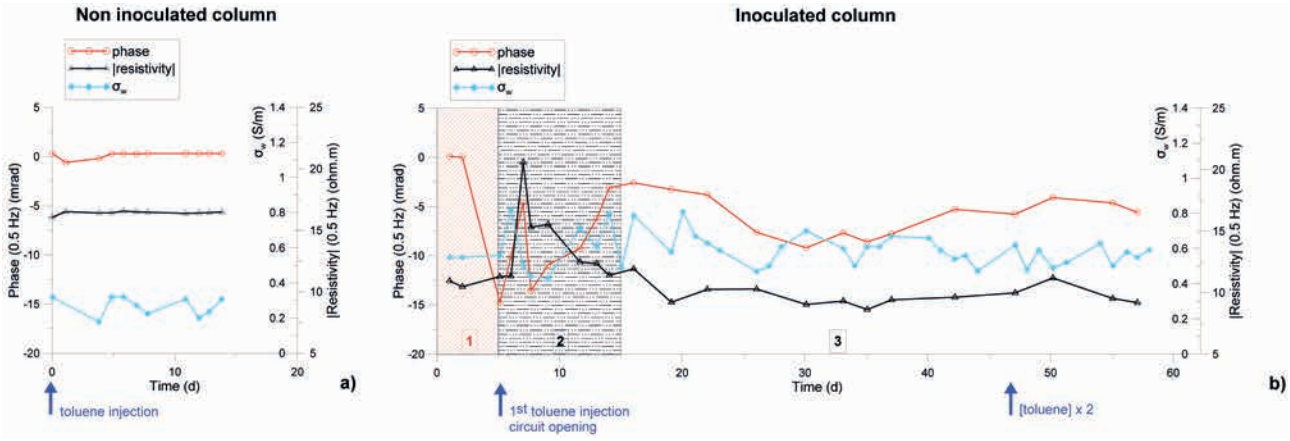

Figure 5 SIP results for the (left) non-inoculated and (right) inoculated columns presented in terms of (a and b) resistivity magnitude and phase shift at 0.5 Hz, as well as the fluid conductivity σ_w measured at the column outlet. Areas 1, 2, and 3 correspond to the inoculation period (days 0–5), the period when bacteria were lost after opening circuit (days 5–15), and the period of biofilm growth (days 15 to the end).

performed before $\delta^{13}C(CO_2)$ determination derived from Keeling plot method (Pataki *et al*. 2003). The $\delta^{13}C(CO_2)$ calibration value is checked just afterward. A certified compressed air gas cylinder ($\delta^{13}C(CO_2)$ = -10.2‰) is used to regularly check this accuracy in the upper data range of isotopic deviation.

Temperature, pH, redox potential (Pt/Ag–AgCl), conductivity, and dissolved oxygen content in the fluid were continuously measured using probes (Mettler Toledo) immediately at the column outlet.

Fluid samples were collected at three levels of the columns (S1, S2, and S3). They were used for (i) daily toluene quantification and (ii) microbial counting of planktonic bacteria three times a week. Bacteria were observed and counted in a Thoma cell with an optical microscope (Zeiss Axio Imager Z1, Göttingen, Germany).

Once a week, some sand was sampled at the top of the inoculated column and strongly vortexed for five minutes in a NaCl 9 $g.L^{-1}$ solution in order to detach the biofilm. Bacteria were enumerated in the supernatant (Fig. 3). At the end, both columns were sampled at different levels for more analyses (counting, DNA analyses).

RESULTS AND DISCUSSION

Results

Microbiological and geochemical results are shown in Fig. 4. The evolution of bacterial densities in the liquid phase of the columns at three different levels is shown in Figs. 4a and 4b. The bacterial concentration remained low in the non-inoculated column (< 10^6 bact/mL, detection limit of Thoma cell counting) due to regular bactericide injections (500 mL per week of water-based solution called formalin, which is 37% formaldehyde by weight). Whereas, in the inoculated column, the cell concentration in the fluid was high (up to 3.10^8 bact/mL) and an increase in the bacterial concentration fixed on the sand was observed during the experiment. A decrease in planktonic bacteria number in the column levels at circuit opening (day 5) can be noted, but the population restarted to grow at day 15. This allows us to delimitate three periods for the inoculated experiment (Fig. 4b): (1) inoculation period, with a high planktonic bacterial population (days 0–5); (2) the period just after circuit opening, when a lot of planktonic bacteria were lost (days 5–15); and (3) the period of biofilm growth, with increase in bacterial population, planktonic, and sessile (days 15–58). It should also be noticed that a mixed bacterial community including *R. wratislaviensis* developed in the inoculated column because pure culture was not achieved throughout the experiment. We decided to inoculate the active column in order to ensure toluene degradation but not to work with pure culture.

Toluene quantification is represented in Figs. 4c and 4d. Toluene concentration was measured in the fluid at different levels of the columns, and it has been chosen to calculate the cumulated quantity lost in the liquid phase, that means the sum of toluene quantities measured at the entry fewer quantities measured at the exit. It showed that little toluene was lost in the non-inoculated column. These few losses should be due to degassing in the air phase (toluene is a volatile compound). However, these losses were negligible in comparison with the losses of toluene occurred into the inoculated column, where toluene was added regularly after its degradation in the column (270 mg/L every three days between day 5 and day 47 and 540 mg/L every three days after day 47).

CO_2 analyses (Figs. 4e and 4f) indicate that toluene was biodegraded into the inoculated column only. Indeed, in the non-inoculated column, CO_2 concentrations stayed around 500 ppmV, which is the ambient air CO_2 concentration level. By contrast, in the inoculated column, a three-step CO_2 production was observed. First, there was a strong increase in CO_2 concentrations, from 500 ppmV to 18000 ppmV, in five days (inoculation period). Then, after opening the circuit, CO_2 concentrations declined to reach a value of 5000 ppmV when planktonic bacteria were lost and rose again progressively up to 30000 ppmV during the biofilm growth. The same three periods delimited previously (1, 2, and 3) fit the

CO_2 data. Moreover, carbon isotopic ratio of this CO_2, $\delta^{13}C(CO_2)$, decreased from -13.6‰, which corresponds to the ambient air CO_2 signature (Boutton 1991), to reach ratios lower than -30.9‰, which is the toluene signature ($\delta^{13}C$ (toluene source) = -30,9 ± 0.4‰, determined by gas chromatography combustion isotope ratio mass spectrometry (GC/C/IRMS)). This confirms that produced CO_2 really resulted from toluene degradation.

Furthermore, if isotopic results are more closely analysed, an isotope fractionation of carbon could be detected during the biodegradation process. Indeed, $\delta^{13}C$ (toluene) was decreasing from -30.5 ± 0.4‰ (day 1) to -28.6 ± 0.4‰ (day 34) (isotopic fractionation of -2.3‰/$\delta^{13}C$(toluene source)), whereas $\delta^{13}C(CO_2)$ is increasing from -13.6 ± 0.6‰ (day 1) to -33.3 ± 0.4‰ (day 28) (isotopic fractionation of +2.4‰ / $\delta^{13}C$ (toluene source)).

The SIP measurements are shown in Figs. 5 and 6. The temporal variation at single frequency (0.5 Hz) is displayed in Fig. 5, and the frequency dependence of measured data is shown in Fig. 6. We focus on a low frequency in Fig. 5 as the peak of relaxation frequency seems to be lower than 0.1 Hz (Fig. 6). In addition, 0.5 Hz is also close to typical frequencies used in field electrical measurements, and this was a frequency at which our measurement error was low.

Temporal evolutions of SIP measurements are displayed as complex resistivity phase and magnitude at 0.5 Hz (Figs. 5a and 5b). The temporal evolution of phase shift ϕ in the non-inoculated column showed no variation, staying around 0 mrad during all the experiments (Fig. 5a). Conversely, in the inoculated column, the phase shift varied (Fig. 5b). It rose from 0 mrad to -15 mrad during the inoculation step (days 1–5). Conversely, in the inoculated column, the phase shift varied (Fig. 5b). It rose from 0 mrad to -15 mrad during the inoculation step (days 1–5). Consequently to the circuit opening and the loss of planktonic bacteria, phase shift decreased (days 7–15, from -13.6 mrad to -2.6 mrad) and then increased again during the biofilm growth (days 30–60, with a maximum at -9.2 mrad at day 30). We drew the same three

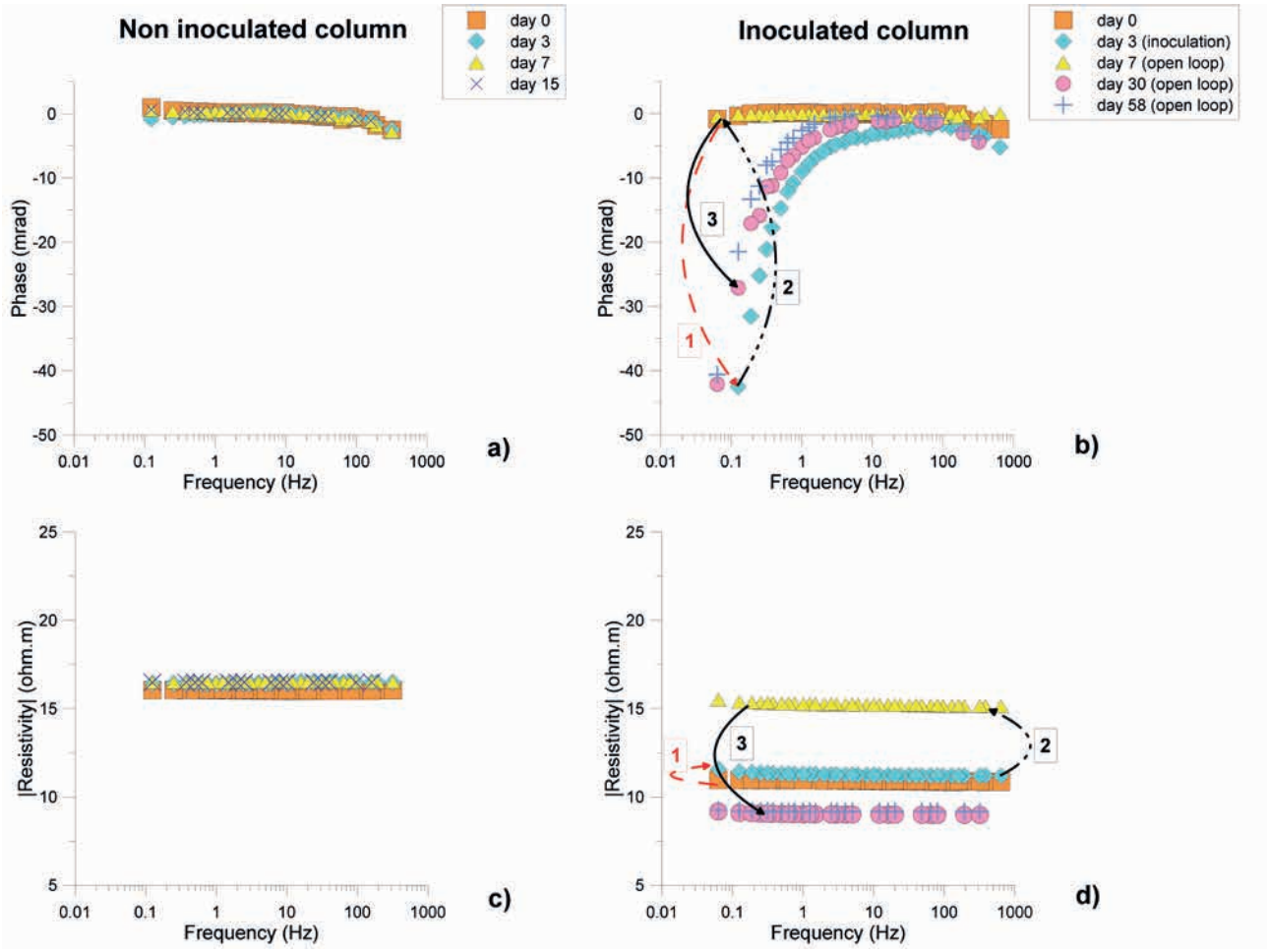

Figure 6 Full spectra of the phase shift between the injected current and the measured voltage (a and b) and resistivity (c and d) measured in the non-inoculated (left) and inoculated (right) columns at different times of the experiments. Arrows 1, 2, and 3 correspond to the transition between days 0 and 3 (inoculation period); to the transition between the inoculation period and the open-loop period (between days 3 and 7); and to the transition towards the period of biofilm growth (days 7 to the end).

periods (1, 2, and 3) delimitated before in Fig. 5b. The resistivity magnitude $|\rho^*(\omega)|$ response in the non-inoculated column was flat, and in the inoculated column, it showed an increase after circuit opening, from 10 Ωm to 15/22 Ωm (comparable with the resistivity of the non-inoculated column) and then a steady decrease to 10 Ωm, lower than initial values. The fluid conductivity σ_w showed alternative variations for both columns between $5.5.10^{-1}$ S/m and 8.10^{-1} S/m. Nonetheless, the deviation in the non-inoculated column was significantly less and seemed to have no effect on resistivity magnitude $|\rho^*(\omega)|$. For the inoculated column, there was a direct link between fluid conductivity and measured resistivity, especially after day 15.

Spectral information is given in Fig. 6 where SIP measurements are displayed as full spectra of phase shift and resistivity. Phase and resistivity spectra are flat and show few variations for the non-inoculated experiment (Figs. 6a and 6c). The three different periods (1, 2, and 3) can be observed for the inoculated column (Figs. 6b and 6d). Moreover, it can be noticed that the phase response is more and more enhanced at lower frequencies (< 10 Hz).

Potential electrode checking

At the end of the inoculated column experiment (60-day duration), the handmade potential electrodes $Cu/CuSO_4$ were checked for reliability. The SIP response was measured in clean sand saturated with tap water and compared with the base line of the inoculated experiment (clean sand + bacterial growth media). A small shift between the two phase spectra was observed, around 3 mrad at 0.5 Hz, which remained lower than the phase variation measured during biodegradation (between 5 mrad and 15 mrad).

Discussion

The microbiological analyses confirmed that a biofilm developed in the inoculated column but not in the non-inoculated control. Geochemical monitoring, especially relative to the CO_2 production and its carbon isotopic signature, showed that the bacterial activity was significant in the inoculated column and not in the non-inoculated column. Indeed, CO_2 was produced in the inoculated column and it showed a very negative isotopic signature (less than -31‰) compared with atmospheric CO_2 (around -11‰). This proves that toluene, with $\delta^{13}C$ (toluene)=-30.9 ± 0.4‰, was the carbon source of the produced CO_2. Moreover, an isotopic fractionation, around 2‰, was also noticeable. It confirms the biological process of degradation, and it is consistent with the isotopic fractionation found by Meckenstock *et al*. 2004 for example.

Before proceeding further, we discuss here the limited duration of the control experiment. Indeed, the duration of the non-inoculated experiment was only 15 days, as compared with 58 days for the inoculated experiment. It is explained by the difficulty to inhibit bacterial growth in the control system despite the accurate sterilization procedure and the regular formaldehyde injections. However, the CO_2 measurements attest that toluene biodegradation occurred only in the active column since day 5, and we considered that no evolution was expected in the control column.

The geoelectrical response appears to reflect sequential changes occurring in the system, as a result of bacterial population variations and toluene biodegradation. SIP response of inoculated column was mainly visible through the phase shift ϕ. Indeed, phase shift ϕ response of our inoculated column exhibited a temporal variation: ϕ reached a peak of 15 mrad at 0.5 Hz just after inoculation phase. Then, it decreases to increase again during biofilm growing period up to 10 mrad. These results are consistent with those of Personna *et al.* (2013) who studied ethanol biodegradation in columns and observed a similar temporal variation of the ϕ response. They observed a slight increase (up to 1.5 mrad) after microbial inoculation and then a slight decrease and an abrupt jump reaching a peak value of 9 mrad at 0.2 Hz. According to Personna *et al.* (2013), the ϕ response reflected changes occurring in the system as a result of biodegradation processes. However, Personna *et al.* detected only 1.5 mrad phase shift, whereas this experiment recorded 15 mrad during inoculation period (noted 1). This first electrical change may have been caused by the removal of ions in solution during intense microbial respiration or by changes in porosity and pore space tortuosity associated with rapid microbial growth and biofilm formation, but it must have been affected by the change of flow regime when the circuit is open. Nevertheless, the 9.2-mrad phase shift at day 30 cannot be explained with other processes than those linked to toluene biodegradation. Indeed, the flow regime is constant, and the resistivity magnitude $|\rho^{\wedge *}$ (*!*)| shows no important variations. During period 3, the bacterial concentration is high, as well as the produced CO_2, which is a direct consequence of bacterial activity.

The SIP measurements showed that changes in ϕ shift generally paralleled those of the microbial counts, with a close correspondence in decreases and increases in ϕ shift and that of the cell concentration in the inoculated column, particularly at period 3. It suggests that the ϕ response resulted, at least partly, from the microbial growth. Microbial growth involves other processes such as ionic solution changes, mineral dissolution, and/or precipitation of new mineral forms, and all of these phenomena can contribute to the signal. Nevertheless, the increase in microbial cell concentration and ϕ shift observed in the inoculated column (days 15 to the end) may be in whole or in part due to the increased attachment of bacteria to the surface of sand grains and the increased aggregation of cells in biofilms.

The SIP measurements showed temporal variation of resistivity magnitude $|\rho^*(\omega)|$ as well. A peak of resistivity magnitude was observed at the beginning of the experiment (days 7–10). It may be due to CO_2 production and the presence of CO_2 gas, which is highly resistive, in the porous media. However, it is precisely when CO_2 concentration is lower than the resistivity peak is measured. So, the resistivity peak could be due to the first toluene injection that fits with the SIP response spike.

After day 10, the resistivity magnitude progressively decreased up to day 20 when it stayed around 10 Ωm, lower than initial values and values measured in the non-inoculated column. The $|\rho^*(\omega)|$ response can be attributed to removal of ions and changes in pore

space due to bacterial clogging (Abdel Aal, Atekwana, and Atekwana 2010). Indeed, we measured an increase in the formation factor F between the baseline (F = 3.9) and the end of the experiment, where F is found to be 4.6. Assuming that m is constant, it would represent a decrease in porosity of 5%. This is consistent with pore clogging by biofilm, and an enhancement of electrical resistivity. $|\rho^*(\omega)|$ should be linked to bacterial presence as well. Indeed, bacteria, like clays, have a high surface conductivity (Revil *et al.* 2012) and should contribute to enhance bulk conductivity. Furthermore, we used pure quartz silica sand to minimize weathering in the column, and therefore, this does not allow significant changes in $|\rho^*(\omega)|$ as quartz solubility at pH lower than 9.5 is lower than 10^{-4}M (Rimstidt 1997).

Finally, we can assume growing presence of bacteria (Revil *et al.* 2012; Zhang *et al.* 2013) and biofilm formation (Davis *et al.* 2006) but also their activities (ions and organic acids production) (Atekwana and Atekwana 2010) induce the SIP parameters, principally ϕ shift.

CONCLUSION

These results have shown that microbial activity is characterized by CO_2 gas production and carbon isotopic fractionation and also by a temporal evolution of the complex electrical resistivity in correlation with microbiological and chemical analyses. Indeed,

- during the five days of the inoculation period, a high bacterial activity was observed and correlated with the following phenomena (Period 1):
  - a CO_2 gas production with a characteristic isotopic signature, proof of toluene degradation;
  - a phase ϕ shift of 15 mrad;
  - constant $|\rho^*(\omega)|$ values.
- Then, a loss of planktonic bacteria leaded to a decrease in bacterial activity characterized by (period 2):
  - less CO_2 gas production;
  - decrease in phase ϕ shift;
  - increase in $|\rho^*(\omega)|$ with similar values compared with the non-inoculated column.
- During biofilm growth (period 3), shown by the expansion of bacterial population fixed on sand (Figs. 3 and 4b), the bacterial activity increased progressively, growth that was accompanied by:
  - CO_2 gas production again;
  - Phase ϕ shift of 5 mrad–10 mrad;
  - a small decrease in $|\rho^*(\omega)|$ due to the expansion of bacterial population.

On the contrary, the non-inoculated column showed no significant variations in SIP signal and CO_2 gas production.

In conclusion, this laboratory study provided evidence that the aerobic biodegradation of toluene can be monitored through a combination of SIP measurements and CO_2 gas analyses (volumetric content and isotopic signature). The SIP response follows the bacterial population evolution (loss of planktonic bacteria and then biofilm growth on the sand) and the associated bacterial activity (CO_2 production as a consequence of toluene biodegradation). This non-invasive monitoring methodology is innovative as it combines geophysical measurements and gas emission analyses at the ground surface, without recurring to monitoring wells. It has to be adapted and tested on sites in order to suitably monitor the progress of hydrocarbon biodegradation during real full-scale bio-treatments.

ACKNOWLEDGEMENTS

The authors would like to thank the French Research Agency (project BIOPHY, ANR-10-ECOT-014) and the LABEX VOLTAIRE (Excellence Laboratory for Atmosphere, Resources and Environmental interactions study, University of Orléans, Orléans, France) (ANR-10-LABX-100-01) for financial support. The authors would also like to thank all the partners of the BIOPHY project: BRGM, LPC2E, Serpol, and Total, who follow our work.

The LPC2E technical research team is gratefully acknowledged for its contribution to the development of the SPIRIT instrument. Highly technical support from BRGM is greatly appreciated as well.

The authors thank Yves Benoit and Françoise Fayolle (IFPEN) for providing them with the *Rhodococcus wratislaviensis* bacteria. And they thank Véronique Naudet for helpful suggestions.

They thank the editor, Dimitrios Ntarlagiannis and an anonymous reviewer for their constructive comments that helped improve the manuscript.

REFERENCES

Abdel Aal G.Z., Atekwana E.A., Slater L.D. and Atekwana E.A. 2004. Effects of microbial processes on electrolytic and interfacial electrical properties of unconsolidated sediments. *Geophysical Research Letters* **31**(12), L12505, doi: 10.1029/2004gl020030.

Abdel Aal G., Slater L. and Atekwana E.A. 2006. Induced-polarization measurements on unconsolidated sediments from a site of active hydrocarbon biodegradation. *Geophysics* **71**(2), H13–H24, doi: 10.1190/1.2187760.

Abdel Aal G.Z., Atekwana E.A. and Atekwana E.A. 2010. Effect of bioclogging in porous media on complex conductivity signatures. *Journal of Geophysical Research: Biogeosciences* **115**(G3), G00–G07, doi: 10.1029/2009jg001159.

Abdel Aal G.Z. and Atekwana E.A. 2014. Spectral induced polarization (SIP) response of biodegraded oil in porous media. *Geophysical Journal International*, **196**(2), 804–817, doi: 10.1093/gji/ggt416.

Aggarwal P.K. and Hinchee R.E. 1991. Monitoring in situ biodegradation of hydrocarbons by using stable carbon isotopes. *Environmental Science & Technology* **25**(6), 1178–1180, doi: 10.1021/es00018a026.

Albrecht R., Gourry J.C., Simonnot M.O. and Leyval C. 2011. Complex conductivity response to microbial growth and biofilm formation on phenanthrene spiked medium. *Journal of Applied Geophysics* **75**(3), 558–564, doi: 10.1016/j.jappgeo.2011.09.001.

Archie G.E. 1942. The electrical resistivity log as an aid in determining some reservoir characteristics. *Transactions AIME* **146**(1), 54–62.

Atekwana E.A. and Atekwana E.A. 2010. Geophysical signatures of microbial activity at hydrocarbon contaminated sites: a review. *Surveys in Geophysics* **31**(2), 247–283, doi: 10.1007/s10712-009-9089-8.

Atekwana E.A. and Slater L.D. 2009. Biogeophysics: a new frontier in Earth science research. *Reviews of Geophysics* **47**(4), RG4004, doi: 10.1029/2009RG000285.

Auffret M., Labbé D., Thouand G., Greer C.W. and Fayolle-Guichard F. 2009. Degradation of a mixture of hydrocarbons, gasoline, and diesel oil additives by Rhodococcus aetherivorans and Rhodococcus wratislaviensis. *Applied and Environmental Microbiology* **75**(24), 7774–7782, doi: 10.1128/AEM.01117-09.

Bleil D. 1953. Induced polarization: a method of geophysical prospecting. *Geophysics* **18**(3), 636–661.

Boutton T.W. 1991. Stable carbon isotope ratios of natural materials: II. Atmospheric, terrestrial, marine, and freshwater environments. *Carbon Isotope Techniques* **1**, 173.

Cassiani G., Kemna A., Villa A. and Zimmermann E. 2009. Spectral induced polarization for the characterization of free-phase hydrocarbon contamination of sediments with low clay content. *Near Surface Geophysics* **7**(5–6), 547–562, doi: 10.3997/1873-0604.2009028.

Das N. and Chandran P. 2011. Microbial degradation of petroleum hydrocarbon contaminants: an overview. *Biotechnology Research International* 941810, doi: 10.4061/2011/941810.

Davis C.A., Atekwana E.A., Atekwana E.A., Slater L.D., Rossbach S. and Mormile M.R. 2006. Microbial growth and biofilm formation in geologic media is detected with complex conductivity measurements. *Geophysical Research Letters* **33**(18), L18403, doi: 10.1029/2006GL027312.

Davis G.B., Laslett D., Patterson B.M. and Johnston C.D. 2013. Integrating spatial and temporal oxygen data to improve the quantification of in situ petroleum biodegradation rates. *Journal of Environmental Management* **117**(15), 42–49, doi: 10.1016/j.jenvman.2012.12.027.

Elsner M. 2010. Stable isotope fractionation to investigate natural transformation mechanisms of organic contaminants: principles, prospects and limitations. *Journal of Environmental Monitoring* **12**, 2005–2031, doi: 10.1039/c0em00277a.

European Commission. 2014. Commission Directive 2014/80/EU, amending Annex II to Directive 2006/118/EC of the European Parliament and of the Council on the protection of groundwater against pollution and deterioration. *Official Journal of the European Union*, L182/52.

Flores Orozco A., Kemna A., Oberdörster C., Zschornack L., Leven C., Dietrich P. *et al*. 2012. Delineation of subsurface hydrocarbon contamination at a former hydrogenation plant using spectral induced polarization imaging. *Journal of Contaminant Hydrology* **136–137**(0), 131–144, doi: 10.1016/j.jconhyd.2012.06.001.

Gogo S., Guimbaud C., Laggoun-Défarge F., Catoire V. and Robert C. 2011. In situ quantification of CH4 bubbling events from a peat soil using a new infrared laser spectrometer. *Journal of Soils and Sediments* **11**(4), 545–551, doi: 10.1007/s11368-011-0338-3.

Guimbaud C., Catoire V., Gogo S., Robert C., Chartier M., Laggoun-Défarge F. *et al*. 2011. A portable infrared laser spectrometer for flux measurements of trace gases at the geosphere–atmosphere interface. *Measurement Science and Technology* **22**(7), 075601, doi: 10.1088/0957-0233/22/7/075601.

Guimbaud C., Noel C., Chartier M., Catoire V., Blessing M., Gourry J.C., Robert C. 2016. A quantum cascade laser infrared spectrometer for CO2 stable isotope analysis: field implementation at a hydrocarbon contaminated site under bio-remediation. *Journal of Environmental Sciences, special issue "Changing complexity of air pollution"*, 40, 60–74, doi:10.1016/j.jes.2015.11.015

Heenan J., Porter A., Ntarlagiannis D., Young L.Y., Werkema D.D. and Slater L.D. 2013. Sensitivity of the spectral induced polarization method to microbial enhanced oil recovery processes. *Geophysics* **78**(5), E261–E269, doi: 10.1190/geo2013-0085.1.

Hunkeler D., Andersen N., Aravena R., Bernasconi S.M. and Butler B.J. 2001. Hydrogen and carbon isotope fractionation during aerobic biodegradation of benzene. *Environmental Science & Technology* **35**(17), 3462–3467, doi: 10.1021/es0105111.

Hyman M. and Dupont R.R. 2001. *Groundwater and Soil Remediation, Process Design and Cost Estimating of Proven Technologies*. Reston, VA: ASCE Press, 534 pp.

Kaufmann K., Christophersen V., Buttler A., Harms H. and Höhener P. 2004. Microbial community response to petroleum hydrocarbon contamination in the unsaturated zone at the experimental field site Værløse, Denmark. *FEMS Microbiology Ecology* **48**(3), 387–399, doi: 10.1016/j.femsec.2004.02.011.

Kemna A., Binley A., Cassiani G., Niederleithinger E., Revil A., Slater D.L. *et al*. 2012. An overview of the spectral induced polarization method for near-surface applications. *Near Surface Geophysics* **10**, 453–468, doi: 10.3997/1873-0604.2012027.

Lessar J.F., Cobian K.E., McIntyre P.B. and Mayer D.W. 2006. Medical electrical lead conductor formed from modified MP35N alloy. Patent US7138582 B2.

Maineult A., Bernabé Y. and Ackerer P. 2004. Electrical response of flow, diffusion, and advection in a laboratory sand box. *Vadose Zone Journal* **3**(4), 1180–1192, doi: 10.2136/vzj2004.1180.

Majone M., Verdini R., Aulenta F., Rossetti S., Tandoi V., Kalogerakis N. *et al*. 2014. In situ groundwater and sediment bioremediation: barriers and perspectives at European contaminated sites. *New Biotechnology* (available online), doi: 10.1016/j.nbt.2014.02.011.

Meckenstock R.U., Morasch B., Griebler C. and Richnow H.H. 2004. Stable isotope fractionation analysis as a tool to monitor biodegradation in contaminated aquifers. *Journal of Contaminant Hydrol*ogy **75**(3–4), 215–255, doi: 10.1016/j.jconhyd.2004.06.003.

Mewafy F.M., Werkema D.D., Atekwana E.A., Slater L.D., Abdel Aal G., Revil A. *et al*. 2013. Evidence that bio-metallic mineral precipitation enhances the complex conductivity response at a hydrocarbon contaminated site. *Journal of Applied Geophysics* **98**(0), 113–123, doi: 10.1016/j.jappgeo.2013.08.011.

Morasch B., Hunkeler D., Zopfi J., Temime B. and Höhener P. 2011. Intrinsic biodegradation potential of aromatic hydrocarbons in an alluvial aquifer – Potentials and limits of signature metabolite analysis and two stable isotope-based techniques. *Water Research* **45**(15), 4459–4469, doi: 10.1016/j.watres.2011.05.040.

Nadim F., Hoag G.H., Liu S., Carley R.J. and Zack P. 2000. Detection and remediation of soil and aquifer systems contaminated with petroleum products: an overview. *Journal of Petroleum Science and Engineering* **26**(1–4), 169–178, doi: 10.1016/S0920-4105(00)00031-0.

Naudet V. and Revil A. 2005. A sandbox experiment to investigate bacteria-mediated redox processes on self-potential signals. *Geophysical Research Letters* **32**(11), L11405, doi: 10.1029/2005GL022735.

Noel C., Gourry J. C., Deparis J., Blessing M., Ignatiadis I., and Guimbaud C. 2016. Combining Geoelectrical Measurements and CO2 Analyses to Monitor the Enhanced Bioremediation of Hydrocarbon-Contaminated Soils: A Field Implementation. *Applied and Environmental Soil Science*, ID 1480976, doi:10.1155/2016/1480976

Ntarlagiannis D., Yee N. and Slater L. 2005. On the low-frequency electrical polarization of bacterial cells in sands. *Geophysical Research Letters* **32**(24), L24402, doi:10.1029/2005GL024751.

Ntarlagiannis D. and Ferguson A. 2009. SIP response of artificial biofilms. *Geophysics* **74**(1), A1–A5, doi: 10.1190/1.3031514.

Olhoeft G.R. 1986. Direct detection of hydrocarbon and organic chemicals with ground penetrating radar and complex resistivity. *Proceedings NWWA/API Conference Petroleum Hydrocarbons and Organic Chemicals in Ground Water-Prevention, Detection and Restoration.*

Oshetski K.C. 1999. Complex resistivity to evaluate the biooxidation of gold ore. MSc thesis, Colorado School of Mines, USA, 148 pp.

Parkhurst D.L. and Appello C.A.J. 1999. User's Guide to PHREEQC (version 2) - A Computer Program for Speciation, Batch-Reaction, One Dimensional Transport and Inverse Geochemical

Calculation, *USGS Water-Resources Investigations* Report 99–4259 312.

Pataki D.E., Ehleringer J.R., Flanagan L.B., Yakir D., Bowling D.R., Still C.J. *et al*. 2003. The application and interpretation of Keeling plots in terrestrial carbon cycle research. *Global Biogeochemical Cycles* **17**(1), 1022, doi: 10.1029/2001gb001850.

Personna Y.R., Ntarlagiannis D., Slater L., Yee N., O'Brien M. and Hubbard S. 2008. Spectral induced polarization and electrodic potential monitoring of microbially mediated iron sulfide transformations. *Journal of Geophysical Research: Biogeosciences* **113**(G2), G02020, doi: 10.1029/2007JG000614.

Personna Y.R., Slater L., Ntarlagiannis D., Werkema D. and Szabo Z. 2013. Complex resistivity signatures of ethanol biodegradation in porous media. *Journal of Contaminant Hydrology* **153**(0), 37–50, doi: 10.1016/j.jconhyd.2013.07.005.

Revil A., Schmutz M. and Batzle M. 2011. Influence of oil wettability upon spectral induced polarization of oil-bearing sands. *Geophysics* **76**(5), A31–A36, doi: 10.1190/geo2011-0006.1.

Revil A., Atekwana E.A., Zhang C., Jardani A. and Smith S. 2012. A new model for the spectral induced polarization signature of bacterial growth in porous media. *Water Resources Research* **48**(9), doi: 10.1029/2012WR011965.

Reynolds J.M. 2011. *An Introduction to Applied and Environmental Geophysics*. John Wiley & Sons.

Rimstidt J.D. 1997. Quartz solubility at low temperatures. *Geochimica et Cosmochimica Acta* **61**, 2553–2558, doi: 10.1016/S0016-7037(97).

Sauck W.A. 2000. A model for the resistivity structure of LNAPL plumes and their environs in sandy sediments. *Journal of Applied Geophysics* **44**(2–3), 151–165, doi: 10.1016/S0926-9851(99)00021-X.

Schmutz M., Revil A., Vaudelet P., Batzle M., Viñao P.F. and Werkema D.D. 2010. Influence of oil saturation upon spectral induced polarization of oil-bearing sands. *Geophysical Journal International* **183**(1), 211–224, doi: 10.1111/j.1365-246X.2010.04751.x.

Schmutz M., Blondel A. and Revil A. 2012. Saturation dependence of the quadrature conductivity of oil-bearing sands. *Geophysical Research Letters* **39**(3), L03402, doi: 10.1029/2011gl050474.

Schwartz N., Shalem T. and Furman A. 2014. The effect of organic acid on the spectral-induced polarization response of soil. *Geophysical Journal International* (available online), doi: 10.1093/gji/ggt529.

Schweitzer P.A. 2004. *Corrosion Resistance Tables: Metals, Nonmetals, Coatings, Mortars, Plastics, Elastomers, and Linings and Fabrics*, 5th edn. *CRC Press* (Series: Corrosion Technology), 912 pp.

Sihota N.J., Singurindy O. and Mayer K.U. 2011. CO2-efflux measurements for evaluating source zone natural attenuation rates in a petroleum hydrocarbon contaminated aquifer. *Environmental Science & Technology* **45**(2), 482–488, doi: 10.1021/es1032585.

Sihota N.J. and Mayer K.U. 2012. Characterizing vadose zone hydrocarbon biodegradation using carbon dioxide effluxes, isotopes, and reactive transport modeling. *Vadose Zone Journal* **11**(4), doi: 10.2136/vzj2011.0204.

Slater L. and Lesmes D. 2002. IP interpretation in environmental investigations. *Geophysics* **67**(1), 77–88, doi:10.1190/1.1451-353.

Sogade J., Scira-Scappuzzo F., Vichabian Y., Shi W., Rodi W., Lesmes D. *et al*. 2006. Induced-polarization detection and mapping of contaminant plumes. *Geophysics* **71**(3), B75–B84, doi: 10.1190/1.2196873.

Towle J., Anderson R., Pelton W., Olhoeft G. and LaBrecque D. 1985. Direct detection of hydrocarbon contaminants using the induced polarization method. *SEG Technical Program Expanded Abstracts*, 145–147.

Ustra A., Slater L., Ntarlagiannis D. and Elis V. 2012. Spectral induced polarization (SIP) signatures of clayey soils containing toluene. *Near Surface Geophysics* **10**(6), 503–515, doi: 10.3997/1873-0604.2012015.

Vanhala H. 1997. Mapping oil-contaminated sand and till with the spectral induced polarization (SIP) method. *Geophysical Prospecting* **45**(2), 303–326.

Weiss J.V. and Cozzarelli I. 2008. Biodegradation in contaminated aquifers: incorporating microbial/molecular methods. *Groundwater* **46**, 305–322, doi: 10.1111/j.1745-6584.2007.00409.x.

Williams K.H., Kemna A., Wilkins M.J., Druhan J., Arntzen E., N'Guessan A.L. *et al*. 2009. Geophysical monitoring of coupled microbial and geochemical processes during stimulated subsurface bioremediation. *Environmental Science & Technology* **43**(17), 6717–6723, doi: 10.1021/es900855j.

Yang L. 2008. Electrical impedance spectroscopy for detection of bacterial cells in suspensions using interdigitated microelectrodes. *Talanta* **74**(5), 1621–1629, doi: 10.1016/j.talanta.2007.10.018.

Zhang C., Slater L. and Prodan C. 2013. Complex dielectric properties of sulfate-reducing bacteria suspensions. *Geomicrobiology Journal* **30**(6), 490–496, doi: 10.1080/01490451.2012.71999